pubs.acs.org/acschemicalbiology

Letters

Single-Cell Activation of the cAMP-Signaling Pathway in 3D Tissues with FRET-Assisted Two-Photon Activation of bPAC

Tomoaki Kinjo, Tetsuya Watabe, Kenju Kobachi, Kenta Terai,* and Michiyuki Matsuda

Cite This: https://dx.doi.org/10.1021/acschembio.0c00333

Read Online

ACCESS | Metrics & More | Article Recommendations | Supporting Information

ABSTRACT: Bacterial photoactivated adenylyl cyclase (bPAC) has been widely used in signal transduction research. However, due to its low two-photon absorption, bPAC cannot be efficiently activated by two-photon (2P) excitation. Taking advantage of the high two-photon absorption of monomeric teal fluorescent protein 1 (mTFP1), we herein developed 2P-activatable bPAC (2pabPAC), a fusion protein consisting of bPAC and mTFP1. In 2pabPAC, the energy absorbed by mTFP1 excites bPAC by Fürster resonance energy transfer (FRET) at *ca.* 43% efficiency. The light-induced increase in cAMP was monitored by a red-shifted FRET biosensor for PKA. In 3D MDCK cells and mouse liver, PKA was activated at single-cell resolution under a 2P microscope. We found that PKA activation in a single hepatocyte caused PKA activation in neighboring cells, indicating the propagation of PKA activation. Thus, 2pabPAC will provide a versatile platform for controlling the cAMP signaling pathway and investigating cell-to-cell communication *in vivo*.

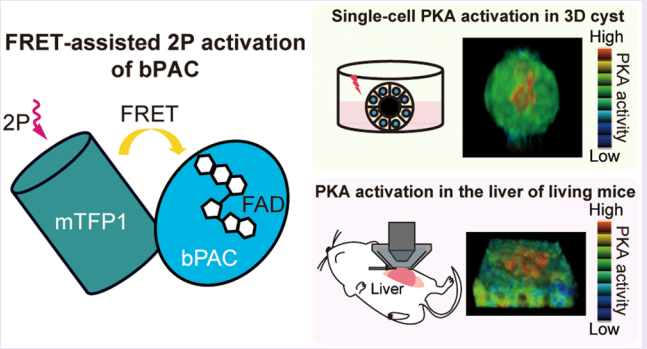

INTRODUCTION

Cyclic adenosine monophosphate (cAMP) is a ubiquitous second messenger regulating multiple cellular processes. Among the downstream effectors of cAMP, cAMP-dependent protein kinase (PKA) has been studied most extensively, and it has been shown to control a number of cellular functions, including glucose metabolism, cell differentiation, sperm motility, hormone secretion, and memory formation.[1] Genetically encoded biosensors based on the principle of Förster resonance energy transfer (FRET) have been developed to visualize spatiotemporal dynamics of the cAMP-PKA pathway, thereby extending our understanding of the complex intracellular and intercellular regulatory mechanisms.[2] cAMP levels have been perturbed by small compounds such as isoproterenol, forskolin, or various cell-permeable cAMP derivatives, enabling temporal control of cAMP/PKA signals *in vitro* and *in vivo*.[3,4] In general, however, these compounds cannot control cells with high spatiotemporal resolution, and thus they are not suitable for investigating the precise characterization of cellular signaling networks.

Flavoprotein-based optogenetic tools offer the means to overcome these problems associated with chemical compounds. A bacterial photoactivated adenylyl cyclase from the filamentous bacterium *Beggiatoa sp.* (bPAC) is an adenylyl cyclase directly linked to a BLUF (blue light receptor using flavin adenine dinucleotide, FAD)-type light sensor.[5] This optogenetic tool permits rapid production of cAMP within cells and has been applied to various types of cells and animals.[6,7]

Two-photon (2P) absorption is a nonlinear optical process that depends on the square of the light intensity, enabling confined excitation of the molecules in the vicinity of the focal plane.[8] This property allows us to develop two-photon excitation microscopy (2PEM), which enables deep tissue fluorescence imaging. However, flavoprotein-based optogenetic tools cannot be efficiently activated by 2P excitation because of the low 2P absorption cross-section (σ_2) of FAD or flavin mononucleotide (FMN).[9] In fact, to the best of our knowledge, there has been no report on the application of bPAC to 2PEM. To overcome the small σ_2 of flavoproteins, we recently developed the FRET-assisted photoactivation (FRAPA) technique, which takes advantage of the large σ_2 of fluorescent proteins to efficiently activate optogenetics tools via FRET from 2P-excited fluorescent proteins.

In this study, we developed 2P-activatable bPAC (2pabPAC), a fusion protein consisting of bPAC and mTFP1 based on the FRAPA technique. We also demonstrate that the cAMP-PKA signaling pathway can be activated with 2pabPAC in the liver of living mice.

Received: April 28, 2020
Accepted: October 12, 2020

RESULTS AND DISCUSSION

We applied the FRAPA technique to bPAC (Figure 1A). We employed mTFP1 as the donor of energy transfer to bPAC because of its large σ_2 and emission spectrum overlap with the absorption of FAD.[9] We generated a series of chimeric proteins consisting of mTFP1 and bPAC and examined the FRET efficiency by fluorescence lifetime imaging microscopy (FLIM;[10] Figure 1B and C). The FRET efficiency depends on the distance and relative orientation between the donor and acceptor chromophores.[11] To minimize the distance, we first trimmed the carboxyl-terminus of mTFP1. On the basis of the crystal structure of mTFP1 (PDB: 2HQK),[12] we found that the 11 amino acids from the C terminus can be deleted without impairing the fluorescence lifetime of mTFP1 (Figure 1C, mTFP1 vs mTFP1ΔC11). Similarly, based on the structure of bPAC (PDB: 5M2A),[13] we found that the first amino acid of the N terminus could be deleted without disturbing light-inducible cAMP production by bPAC. Thus, we fused mTFP1 with a 10 or 11 amino acid deletion (mTFP1ΔC10 or ΔC11) to bPAC with or without an amino acid deletion (bPAC or bPACΔN1), generating four fusion proteins (Figure 1C). Among these four fusion proteins, mTFP1ΔC11-bPAC exhibited the largest decrease in fluorescence lifetime, from 2.8 to 1.6 ns, and, therefore, was renamed as 2pabPAC (Figure 1B, C). We also tested circular permutation variants of mTFP1 for changing the topology of the donor and the acceptor. However, we concluded that the slightly higher FRET efficiency in cp229-bPACΔN1 would not provide a significant advantage because of its reduction in fluorescence and maturation speed.[14]

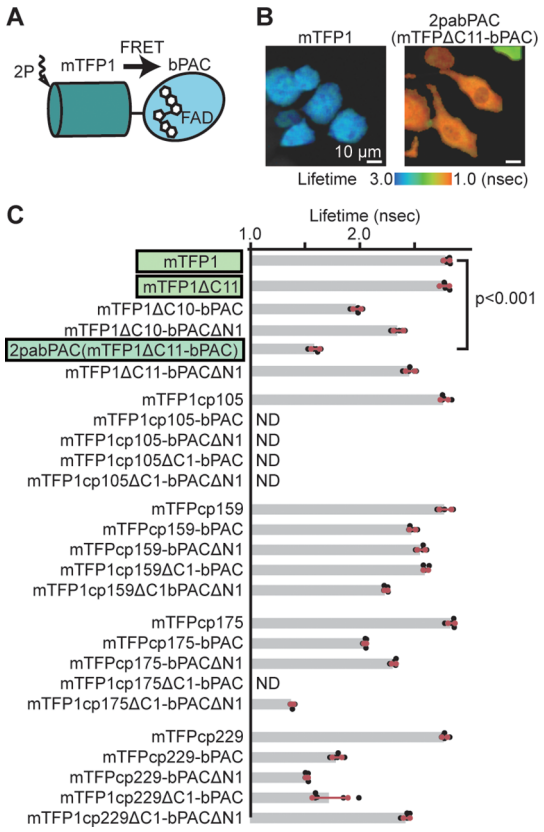

Figure 1. Fluorescence lifetime of 2pabPAC. (A) Scheme of FRET-assisted photoactivation of bPAC. (B) Representative fluorescence lifetime images of Hela cells expressing mTFP1 alone or 2pabPAC, a fusion protein consisting of mTFP1ΔC11 and bPAC. Scale bars, 10 μm. (C) Fluorescence lifetime of mTFP1 variants or the indicated chimeric proteins in HeLa cells. The bar graphs show the mean values. n = 5 cells for each protein; error bars represent the s.d. ND, no detectable fluorescence; two-tailed t tests were used for p-value calculations.

The FRET efficiency of 2pabPAC calculated from the reduction of fluorescence lifetime is 43%. With this value, we could estimate the enhancement of bPAC activation. On the basis of the two level approximation model,[15,16] the σ2 is typically proportional to the square of molar extinction coefficient (ε) in noncentrosymmetric dipolar chromophores such as FAD. Because the 1P absorption spectrum of FAD is almost identical with that of FMN, the σ2 of FAD can be approximated with the σ2 of FMN, one Goeppert−Mayer (GM) unit for the S0−S1 transition.[17] In agreement with this assumption, it is reported that the two-photon absorption of FMN and FAD is at a similar level.[18] Since the σ_2 of mTFP1 is *ca.* 70 GM,[19] the apparent σ2 of 2pabPAC, 30 GM, is obtained by multiplying 70 GM by 43% FRET efficiency from mTFP1 to bPAC. Thus, the 2P absorption efficiency of 2pabPAC is estimated to be approximately 30-fold larger than that of the authentic bPAC.

This successful development of 2pabPAC might be attributable to the small molecular size of bPAC. The molecular size of bPAC, 33 kDa, is less than half that of other flavoprotein-based optogenetic tools, such as CRY2 (70 kDa)[20] and FKF1 (70 kDa).[21] Accordingly, the distance from the amino-terminus to the chromophore is 2.09 nm for bPAC, which is approximately half that of CRY2, 4.07 nm.[13,22] Thus, we expect that FRAPA could also be applicable to other small-sized photoactivatable flavoproteins, such as VVD and Magnets.[23,24]

Does 2pabPAC indeed increase cAMP production by 2P excitation? To confirm this, we monitored PKA activity with Booster-PKA, a red-shifted FRET biosensor for PKA[25] (Figure 2A). As a negative control of 2pabPAC, we generated 2pabPAC(Y72L), in which Tyr[72] of mTFP1, a residue essential for chromophore formation,[26] was replaced with Leu. HeLa cells stably expressing Booster-PKA were transfected with a plasmid encoding 2pabPAC-P2A-mTFP1 or 2pabPAC(Y72L)-P2A-mTFP1. The mTFP1 following the P2A peptide was used to monitor the expression level of 2pabPAC and 2pabPAC-(Y72L). Fluorescence images of HeLa cells were acquired with a 2P microscope at a wavelength of 1040 nm (11 mW, 0.828 μm pixel^{-1}, 2 μs pixel^{-1}, every 10 s). For the photoactivation of 2pabPAC, cells were exposed iteratively at 870 nm (3 mW, 0.828 μm pixel^{-1}, 2 μs pixel^{-1}, 20 scans, every 10 s; Figure 2B). Notably, overexpression of 2pabPAC or 2pabPAC(Y72L) raised the basal PKA activity signal in the absence of light stimulation (Figure 2C); therefore, we chose cells expressing a modest level of 2pabPAC for the following analyses. The PKA activity in 2pabPAC-expressing cells was increased rapidly after 2P activation to a similar extent as that after single-photon (1P) excitation, indicating efficient PKA activation (Figure 2D,E). In 2pabPAC(Y72L)-expressing cells, PKA was activated only by 1P excitation (470 nm, 3.3−6.2 mW cm^{-2} for 3 s). Notably, the σ2 of mTFP1 at 1040 nm is very low;[19] therefore, we did not detect any PKA activation by 2pabPAC during observation of Booster-PKA at 1040 nm.

How much exposure is enough for 2pabPAC function? Under our experimental conditions, 3 mW (870 nm, 0.828 μm

https://dx.doi.org/10.1021/acschembio.0c00333
ACS Chem. Biol. XXXX, XXX, XXX−XXX

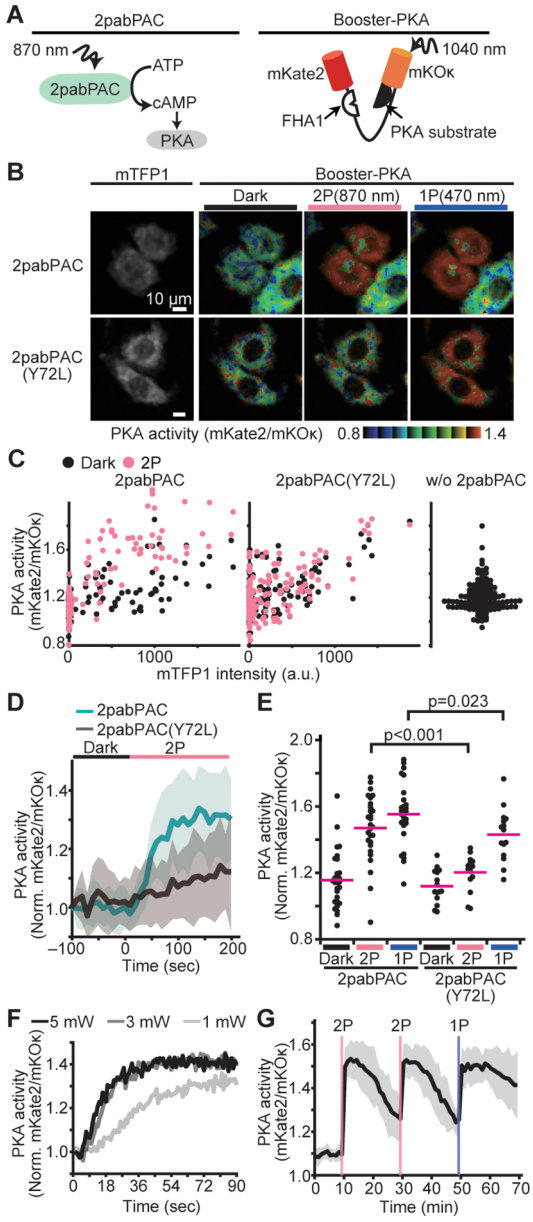

Figure 2. PKA activation by 2pabPAC. (A) Scheme of the experimental design. 2pabPAC was activated at 870 nm, and bPAC-mediated PKA activation was monitored with Booster-PKA at 1040 nm. (B–E) PKA activation by 2P excitation. HeLa cells expressing Booster-PKA were coexpressed with or without 2pabPAC-P2A-mTFP1 or 2pabPAC(Y72L)-P2A-mTFP1 and irradiated with 2P or 1P. Scale bars, 10 μm. The representative images of PKA activity are shown in the IMD mode (B, C). The averaged PKA activity normalized by the mKate2/mKOκ values before stimulation is plotted as a function of time with the s.d.; n = 28 cells for 2pabPAC and n = 15 cells for 2pabPAC(Y72L) (D). Bee swarm plots show the PKA activity before and 100 s after 2P activation; scale bars, 10 μm. Red lines, mean; two-tailed t tests were used for comparison (E). (F) Dose-dependent activation of PKA. HeLa cells expressing 2pabPAC and Booster-PKA were irradiated with the indicated power. The averaged mKate2/mKOκ values were plotted for more than 11 samples from three independent experiments. (G) Repeatability of 2pabPAC. HeLa cells expressing Booster-PKA and 2pabPAC were kept under dark conditions for at least 1 h. For FRET imaging, cells were imaged under the following conditions: 1040 nm, 11 mW, 0.414 μm pixel^{-1}, 2 μs pixel^{-1}, every 1 min. The averaged mKate2/mKOκ values with the s.d. were plotted from six cells.

pixel^{-1}, 2 μs pixel^{-1}, every 0.9 s, 27 scans) was sufficient to achieve the maximum PKA activation in Booster-PKA (Figure 2F). The half-maximum activation is achieved approximately at 15 s after stimulation. Although the peak of PKA activation appeared late, these gaps might be explainable by the kinetics from the cAMP induction to the substrate phosphorylation by PKA. These values are consistent with a previous report about *Xenopus* oocytes expressing bPAC.[5]

We further tested the reversibility and repeatability of the 2pabPAC. For the photoactivation of 2pabPAC, cells were exposed to short pulses of 2P activation (870 nm, 5 mW, 0.414 μm pixel^{-1}, 2 μs pixel^{-1}, 10 scans in 10 s) and 1P activation. PKA activity was increased after short pulses of stimulation and spontaneously decreased under dark conditions (Supporting Figure 1). Under these conditions, the half-life of PKA activity monitored by Booster-PKA was 6.4 min in HeLa cells. This photoactivation/inactivation cycle was repeatable (Figure 2G). As will be described later, the decay of 2pabPAC-stimulated PKA activity is markedly faster in mouse hepatocytes. Therefore, the decay constant observed by PKA activity appears to reflect the decay constant of either phosphodiesterase-mediated cAMP decrease or protein phosphatase-mediated dephosphorylation of Booster-PKA but not 2pabPAC.

A unique advantage of 2PEM is the ability to excite fluorophores at single-cell resolution in 3D space.[8] To demonstrate that 2pabPAC indeed induces PKA activation at single-cell resolution in 3D space, we prepared MDCK cells stably expressing Booster-PKA and 2pabPAC. Cells plated on Matrigel formed cysts with a central cavity (Figure 3A). Upon 2P activation of a single cell (870 nm, 5 mW, 0.497 μm pixel^{-1}, 2 μs pixel^{-1}, 40 scans), a rapid and robust increase in the mKate2/mKOκ ratio was observed only in the irradiated cell, demonstrating the PKA activation at single-cell resolution in a 3D cyst (Figure 3A,B). The same cyst was illuminated with blue light to confirm that PKA could be activated in almost all cells in a bPAC-dependent manner (Figure 3A,B). We also quantified the PKA activation by 2pabPAC in MDCK cysts with or without 2pabPAC. Upon 2P excitation (870 nm, 5 mW, 0.497 μm pixel^{-1}, 2 μs pixel^{-1}, 20 scans), a robust PKA activation was observed in the cysts expressing Booster-PKA and 2pabPAC, while the cysts expressing Booster-PKA without 2pabPAC showed a marginal change under 2P activation (Figure 3C). These results confirmed that 2pabPAC allows us to generate cAMP at the single-cell resolution in 3D space. We performed a similar experiment with MDCK cysts expressing 2pabPAC and Booster-ERK, a red-shifted biosensor for external signal-regulated kinase (ERK),[25] but no apparent changes in the mKate2/mKOκ ratio were observed, indicating the specificity of 2pabPAC to the cAMP signaling pathway (Figure 3D).

Finally, we applied 2pabPAC for *in vivo* control of PKA activity. Previously, we reported that activation of ERK propagates to the neighboring cells in the epidermis.[27] Propagation of PKA activation was also found in culture cells.[25] However, it remains unknown whether PKA activation propagates to the neighboring cells in living tissues. To explore this possibility, we attempted visualization and optical control of the PKA activity in living mice. We focused on the liver because the cAMP-PKA signaling pathway regulates various functions in the liver, including lipid metabolism, inflammation, and cell differentiation.[28] To deliver 2pabPAC into mouse hepatocytes, we utilized an AAV2/8 vector, AAV2 pseudoserotyped with the type 8 capsid, because of efficient liver

https://dx.doi.org/10.1021/acschembio.0c00333
ACS Chem. Biol. XXXX, XXX, XXX−XXX

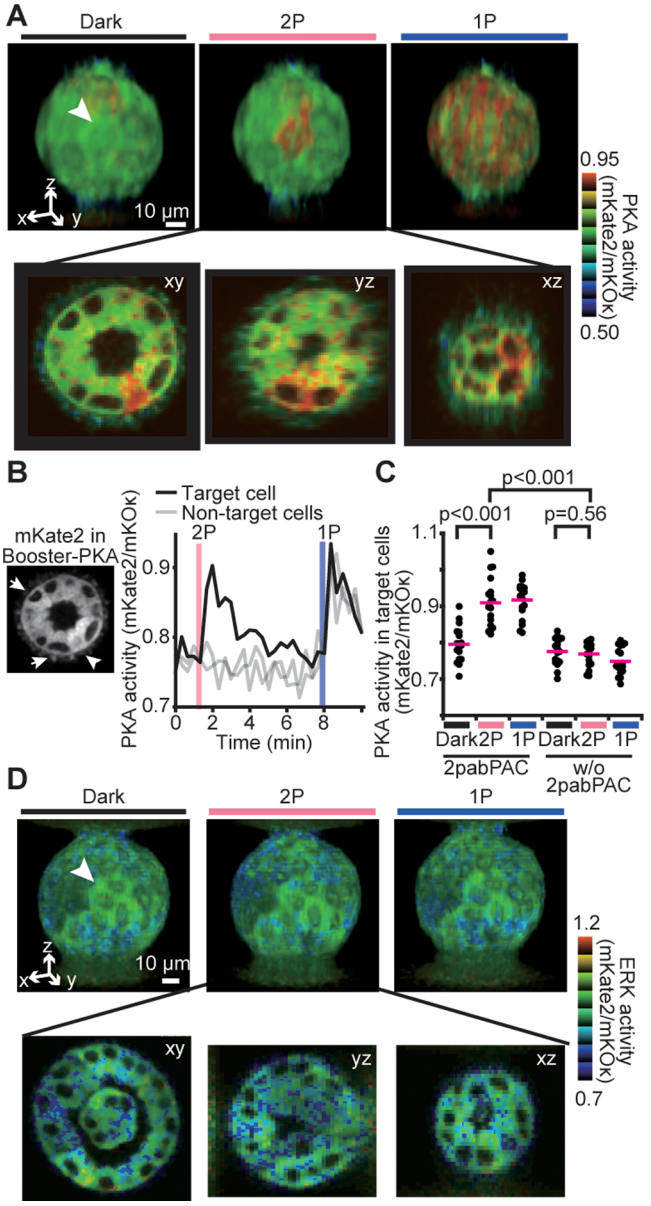

Figure 3. Single-cell control of PKA activity in the 3D epithelial cyst. (A) Representative 3D images of the MDCK cyst under dark conditions, 20 s after single-cell 2pabPAC activation by 2P excitation, and whole-cell activation by 1P excitation. An arrowhead in the upper-left panel indicates the target cell of 2P excitation. 2D section images in the *xy*, *yz*, and *xz* planes are also shown in the lower panels. (B) Time courses of PKA activity in the target cell (arrowhead) and two representative nontarget cells (arrows). 2pabPAC in the target cell was activated by 2P excitation at 1.3 min, and then reactivated by 1P excitation at 8.0 min. The peaks just after activation are plotted in the right panel. (C) Quantification of PKA activation by 2pabPAC. MDCK cysts with or without 2pabPAC were activated by 2P and 1P excitation. Bee swarm plots show the PKA activity before and after 2P or 1P activation; n = 18 cells in six cysts from three independent experiments. The red lines represent the average values. Two-tailed t tests were used for p value calculations. (D) Negative control for 2pabPAC. Experiments similar to those depicted in A were performed in MDCK cells expressing Booster-ERK and 2pabPAC.

transduction.[29] The recombinant virus carrying 2pabPAC-P2A-mTFP1 was injected intraperitoneally into EIIa-cre/lox-Booster-PKAchu mice, which ubiquitously expresses Booster-PKA.[25] After a more than 3-day-incubation period, the liver was immobilized with a custom-made vacuum-stabilized imaging window and observed with a 2P microscope. Upon 2P activation of a single cell (870 nm, 10−13 mW, 0.497−0.795 μm pixel^{-1}, 2 μs pixel^{-1}, 10 scans), a rapid and robust increase in the mKate2/mKOκ ratio similar to that induced by 1P excitation was observed (Figure 4A). Meanwhile, the

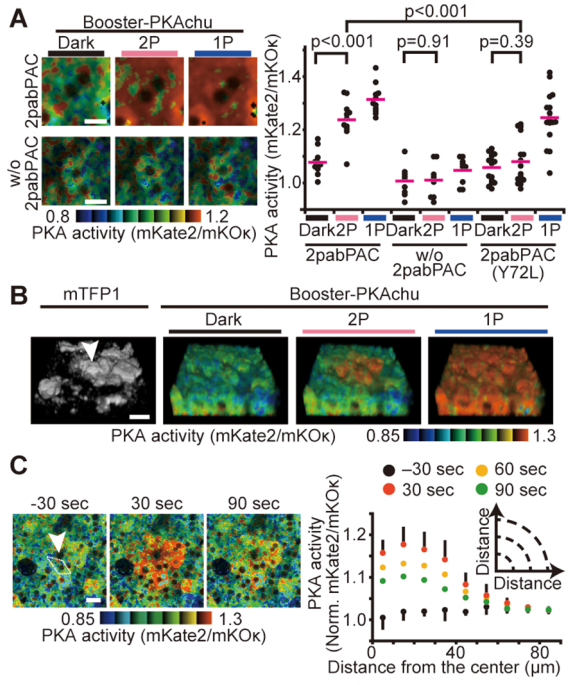

Figure 4. 2P activation of PKA *in vivo*. (A) Representative FRET images of the hepatocytes. The livers of Booster-PKAchu mice with or without 2pabPAC expression were imaged under dark conditions, and then at 30 s after single-cell activation by 2P excitation or 1P excitation (480 nm, 6.8 mW cm^{-2}, 3 s). The right panel shows the quantitated results for 2pabPAC; 11 cells from six individual mice, without 2pabPAC; nine cells from three individual mice, and 2pabPAC(Y72L); 16 cells from three individual mice. The red lines represent the average values. Scale bar: 10 μm. Two-tailed t tests were used for p value calculations. (B) The propagation of PKA activation. Experiments similar to those described in A were performed in a Booster-PKAchu mouse expressing 2pabPAC. A 3D reconstruction image of mTFP1 represents the 2pabPAC-expressing cells in the IMD mode. An arrowhead in the left panel indicates the target cell of 2P excitation. Scale bar: 20 μm. (C) The spatial and temporal dynamics of PKA activation. The livers of Booster-PKAchu mice with 2pabPAC expression were imaged at the indicated time points. The PKA activities of the target cells (arrowhead) and those of the surrounding cells were measured and are shown with the distance from the center of the target cells. Scale bar: 20 μm; error bars represent the s.d. n = 8 experiments from six individual mice.

control mice, which expressed Booster-PKA alone with or without 2pabPAC(Y72L), showed no more than a marginal change under 2P excitation, demonstrating that 2pabPAC is effective *in vivo*. Notably, the PKA activation was detected not only in the target cell but also in a few cells juxtaposed to the target cell (Figure 4B), indicating that PKA activity was propagated as in *in vitro* culture cells.[25]

We further investigated the propagation of PKA activity derived from a single cell (Figure 4C). The peak of PKA activation via the centered cell was earlier than 30 s. This activation was limited to about 40 μm. Moreover, after widespread illumination (1P) by a blue flashlight, PKA activity

https://dx.doi.org/10.1021/acschembio.0c00333
ACS Chem. Biol. XXXX, XXX, XXX−XXX

was increased in almost all cells in the viewfield, although 2pabPAC was rarely expressed in all hepatocytes, supporting the notion that PKA activation was propagated from 2pabPAC-expressing cells to the neighboring cells.

How can the PKA activation in a single cell be propagated to the neighboring cells in the liver? Major target molecules of cAMP are as follows: PKA, cAMP-gated ion channel (CNG), phosphodiesterase (PDE), and exchange proteins directly activated by the cAMP/cAMP-activated guanine nucleotide exchange factor (EPAC/cAMP-GEF). To the best of our knowledge, none of these four major cAMP-dependent proteins has been linked to cell-to-cell propagation of PKA activation. Nevertheless, cAMP signaling is known to regulate exocytosis of hormones in a variety of secretory cells, such as pancreatic beta cells and pituitary cells, by modulating intracellular Ca^{2+} concentrations through PKA-dependent and -independent mechanisms.[30] Thus, cAMP-dependent release of signaling molecules might contribute to the propagation of PKA activation between hepatocytes. The exact role of such propagation of PKA activation remains to be studied, but we speculate that by sharing the information among cell populations and thereby responding synchronously, the cells and the organs thereof can respond to external signals efficiently.

In conclusion, we have developed 2pabPAC, a 2P-activatable optogenetic tool, to control cAMP signaling at single-cell resolution *in vivo*. Even though installation of the imaging window requires technical expertise, a combination of 2pabPAC and 2P imaging will be a promising approach to decipher the spatiotemporal dynamics of cAMP signaling in live tissues.

METHODS

For details, see the Supporting Information.

ASSOCIATED CONTENT

Supporting Information

Supplementary movies 1−3, (PDF). The Supporting Information is available free of charge at https://pubs.acs.org/doi/10.1021/acschembio.0c00333.

Methods and nucleotide sequences of 2pabPAC (PDF)

Supplementary movie 1 (AVI)

Supplementary movie 2 (AVI)

Supplementary movie 3 (AVI)

AUTHOR INFORMATION

Corresponding Author

Kenta Terai − *Research Center for Dynamic Living Systems, Graduate School of Biostudies, Kyoto University, Kyoto, Japan;* orcid.org/0000-0001-7638-3720; Email: terai.kenta.5m@kyoto-u.ac.jp

Authors

Tomoaki Kinjo − *Department of Pathology and Biology of Diseases, Graduate School of Medicine, Kyoto University, Kyoto, Japan;* orcid.org/0000-0003-0939-7756

Tetsuya Watabe − *Department of Pathology and Biology of Diseases, Graduate School of Medicine, Kyoto University, Kyoto, Japan;* orcid.org/0000-0002-9561-9679

Kenju Kobachi − *Research Center for Dynamic Living Systems, Graduate School of Biostudies, Kyoto University, Kyoto, Japan*

Michiyuki Matsuda − *Department of Pathology and Biology of Diseases, Graduate School of Medicine and Research Center for Dynamic Living Systems, Graduate School of Biostudies, Kyoto University, Kyoto, Japan*

Complete contact information is available at: https://pubs.acs.org/10.1021/acschembio.0c00333

Author Contributions

T.K., K.T., and M.M. designed the experiments. T.K., K.K., and T.W. performed the experiments. T.K., K.T., and M.M. analyzed the data and wrote the manuscript.

Notes

The authors declare no competing financial interest.

ACKNOWLEDGMENTS

We thank the members of the Matsuda Laboratory for their helpful input and encouragement; K. Hirano, K. Takakura, and Y. Takeshita for their technical assistance; and the Medical Research Support Center of Kyoto University for *in vivo* imaging. This work was supported by JSPS KAKENHI17J07950 (T.K.), JSPS KAKENHI 18K07066 (K.T.), JSPS KAKENHI 19H00993, JSPS KAKENHI 15H05949 "Resonance Bio," JSPS KAKENHI 16H06280 "ABiS," and CRESTJPMJCR1654 (M.M.).

REFERENCES

(1) Krishnamurthy, V. V., Khamo, J. S., Mei, W., Turgeon, A. J., Ashraf, H. M., Mondal, P., Patel, D. B., Risner, N., Cho, E. E., Yang, J., and Zhang, K. (2016) Reversible optogenetic control of kinase activity during differentiation and embryonic development. *Development 143* (21), 4085−4094.

(2) Paramonov, V. M., Mamaeva, V., Sahlgren, C., and Rivero-Muller, A. (2015) Genetically-encoded tools for cAMP probing and modulation in living systems. *Front. Pharmacol. 6*, 196.

(3) Wagoner, P. K., and Pallotta, B. S. (1988) Modulation of acetylcholine receptor desensitization by forskolin is independent of cAMP. *Science 240* (4859), 1655−1657.

(4) Schaap, P., van Ments-Cohen, M., Soede, R., Brandt, R., Firtel, R. A., Dostmann, W., Genieser, H.-G., Jastorff, B., and Van Haastert, P. (1993) Cell-permeable non-hydrolyzable cAMP derivatives as tools for analysis of signaling pathways controlling gene regulation in Dictyostelium. *J. Biol. Chem. 268* (9), 6323−6331.

(5) Stierl, M., Stumpf, P., Udwari, D., Gueta, R., Hagedorn, R., Losi, A., Gartner, W., Petereit, L., Efetova, M., Schwarzel, M., Oertner, T. G., Nagel, G., and Hegemann, P. (2011) Light modulation of cellular cAMP by a small bacterial photoactivated adenylyl cyclase, bPAC, of the soil bacterium Beggiatoa. *J. Biol. Chem. 286* (2), 1181−8.

(6) Patel, N., and Gold, M. G. (2015) The genetically encoded tool set for investigating cAMP: more than the sum of its parts. *Front. Pharmacol. 6*, 164−164.

(7) Jansen, V., Jikeli, J. F., and Wachten, D. (2017) How to control cyclic nucleotide signaling by light. *Curr. Opin. Biotechnol. 48*, 15−20.

(8) Denk, W., Strickler, J. H., and Webb, W. W. (1990) Two-photon laser scanning fluorescence microscopy. *Science 248* (4951), 73−76.

(9) Kinjo, T., Terai, K., Horita, S., Nomura, N., Sumiyama, K., Togashi, K., Iwata, S., and Matsuda, M. (2019) FRET-assisted photoactivation of flavoproteins for in vivo two-photon optogenetics. *Nat. Methods 16* (10), 1029−1036.

(10) Yasuda, R., Harvey, C. D., Zhong, H., Sobczyk, A., van Aelst, L., and Svoboda, K. (2006) Supersensitive Ras activation in dendrites and spines revealed by two-photon fluorescence lifetime imaging. *Nat. Neurosci. 9* (2), 283−91.

(11) Clegg, R. M. (1995) Fluorescence resonance energy transfer. *Curr. Opin. Biotechnol. 6* (1), 103−110.

(12) Ai, H. W., Henderson, J. N., Remington, S. J., and Campbell, R. E. (2006) Directed evolution of a monomeric, bright and photostable

version of Clavularia cyan fluorescent protein: structural characterization and applications in fluorescence imaging. *Biochem. J. 400* (3), 531−40.
(13) Lindner, R., Hartmann, E., Tarnawski, M., Winkler, A., Frey, D., Reinstein, J., Meinhart, A., and Schlichting, I. (2017) Photoactivation Mechanism of a Bacterial Light-Regulated Adenylyl Cyclase. *J. Mol. Biol. 429* (9), 1336−1351.
(14) Fritz, R. D., Letzelter, M., Reimann, A., Martin, K., Fusco, L., Ritsma, L., Ponsioen, B., Fluri, E., Schulte-Merker, S., van Rheenen, J., and Pertz, O. (2013) A Versatile Toolkit to Produce Sensitive FRET Biosensors to Visualize Signaling in Time and Space. *Sci. Signaling 6* (285), rs12−rs12.
(15) Rebane, A., Drobizhev, M., Makarov, N., Beuerman, E., Tillo, S., and Hughes, T. (2010) New all-optical method for measuring molecular permanent dipole moment difference using two-photon absorption spectroscopy. *J. Lumin. 130* (9), 1619−1623.
(16) Drobizhev, M., Meng, F., Rebane, A., Stepanenko, Y., Nickel, E., and Spangler, C. W. (2006) Strong Two-Photon Absorption in New Asymmetrically Substituted Porphyrins: Interference between Charge-Transfer and Intermediate-Resonance Pathways. *J. Phys. Chem. B 110* (20), 9802−9814.
(17) Homans, R. J., Khan, R. U., Andrews, M. B., Kjeldsen, A. E., Natrajan, L. S., Marsden, S., McKenzie, E. A., Christie, J. M., and Jones, A. R. (2018) Two photon spectroscopy and microscopy of the fluorescent flavoprotein, iLOV. *Phys. Chem. Chem. Phys. 20* (25), 16949−16955.
(18) Villabona-Monsalve, J. P., Varnavski, O., Palfey, B. A., and Goodson, T. (2018) Two-Photon Excitation of Flavins and Flavoproteins with Classical and Quantum Light. *J. Am. Chem. Soc. 140* (44), 14562−14566.
(19) Drobizhev, M., Makarov, N. S., Tillo, S. E., Hughes, T. E., and Rebane, A. (2011) Two-photon absorption properties of fluorescent proteins. *Nat. Methods 8* (5), 393−399.
(20) Kennedy, M. J., Hughes, R. M., Peteya, L. A., Schwartz, J. W., Ehlers, M. D., and Tucker, C. L. (2010) Rapid blue-light-mediated induction of protein interactions in living cells. *Nat. Methods 7* (12), 973−5.
(21) Yazawa, M., Sadaghiani, A. M., Hsueh, B., and Dolmetsch, R. E. (2009) Induction of protein-protein interactions in live cells using light. *Nat. Biotechnol. 27*, 941.
(22) Ma, L., Wang, X., Guan, Z., Wang, L., Wang, Y., Zheng, L., Gong, Z., Shen, C., Wang, J., Zhang, D., Liu, Z., and Yin, P. (2020) Structural insights into BIC-mediated inactivation of Arabidopsis cryptochrome 2. *Nat. Struct. Mol. Biol. 27* (5), 472−479.
(23) Wang, X., Chen, X., and Yang, Y. (2012) Spatiotemporal control of gene expression by a light-switchable transgene system. *Nat. Methods 9* (3), 266.
(24) Kawano, F., Suzuki, H., Furuya, A., and Sato, M. (2015) Engineered pairs of distinct photoswitches for optogenetic control of cellular proteins. *Nat. Commun. 6*, 6256.
(25) Watabe, T., Terai, K., Sumiyama, K., and Matsuda, M. (2020) Booster, a Red-Shifted Genetically Encoded Forster Resonance Energy Transfer (FRET) Biosensor Compatible with Cyan Fluorescent Protein/Yellow Fluorescent Protein-Based FRET Biosensors and Blue Light-Responsive Optogenetic Tools. *ACS Sens 5* (3), 719−730.
(26) Rosenow, M. A., Huffman, H. A., Phail, M. E., and Wachter, R. M. (2004) The Crystal Structure of the Y66L Variant of Green Fluorescent Protein Supports a Cyclization−Oxidation−Dehydration Mechanism for Chromophore Maturation. *Biochemistry 43* (15), 4464−4472.
(27) Hiratsuka, T., Fujita, Y., Naoki, H., Aoki, K., Kamioka, Y., and Matsuda, M. (2015) Intercellular propagation of extracellular signal-regulated kinase activation revealed by in vivo imaging of mouse skin. *eLife 4*, No. e05178.
(28) Wahlang, B., McClain, C., Barve, S., and Gobejishvili, L. (2018) Role of cAMP and phosphodiesterase signaling in liver health and disease. *Cell. Signalling 49*, 105−115.
(29) Cunningham, S. C., Dane, A. P., Spinoulas, A., and Alexander, I. E. (2008) Gene delivery to the juvenile mouse liver using AAV2/8 vectors. *Mol. Ther. 16* (6), 1081−8.
(30) Seino, S., and Shibasaki, T. (2005) PKA-dependent and PKA-independent pathways for cAMP-regulated exocytosis. *Physiol. Rev. 85* (4), 1303−42.

https://dx.doi.org/10.1021/acschembio.0c00333
ACS Chem. Biol. XXXX, XXX, XXX−XXX